



First-principles study of surface plasmons on Ag(111) and H/Ag(111)

Yan, Jun; Jacobsen, Karsten Wedel; Thygesen, Kristian Sommer

Published in:
Physical Review B Condensed Matter

Link to article, DOI:
[10.1103/PhysRevB.84.235430](https://doi.org/10.1103/PhysRevB.84.235430)

Publication date:
2011

Document Version
Publisher's PDF, also known as Version of record

[Link back to DTU Orbit](#)

Citation (APA):
Yan, J., Jacobsen, K. W., & Thygesen, K. S. (2011). First-principles study of surface plasmons on Ag(111) and H/Ag(111). *Physical Review B Condensed Matter*, 84(23), 235430. <https://doi.org/10.1103/PhysRevB.84.235430>

General rights

Copyright and moral rights for the publications made accessible in the public portal are retained by the authors and/or other copyright owners and it is a condition of accessing publications that users recognise and abide by the legal requirements associated with these rights.

- Users may download and print one copy of any publication from the public portal for the purpose of private study or research.
- You may not further distribute the material or use it for any profit-making activity or commercial gain
- You may freely distribute the URL identifying the publication in the public portal

If you believe that this document breaches copyright please contact us providing details, and we will remove access to the work immediately and investigate your claim.

First-principles study of surface plasmons on Ag(111) and H/Ag(111)

Jun Yan, Karsten W. Jacobsen, and Kristian S. Thygesen*

Center for Atomic-scale Materials Design, Department of Physics, Technical University of Denmark, DK-2800 Kongens Lyngby, Denmark

(Received 15 November 2011; published 20 December 2011)

Linear-response time-dependent density functional theory is used to investigate the relation between molecular bonding and surface plasmons for the model system H/Ag(111). We employ an orbital-dependent exchange-correlation functional to obtain a correct description of the Ag 3*d* band, which is crucial to avoid overscreening the plasmon by the *s-d* interband transitions. For the clean surface, this approach reproduces the experimental plasmon energies and dispersion to within 0.15 eV. Adsorption of hydrogen shifts and damps the Ag(111) surface plasmon and induces a new peak in the loss function at 0.6 eV below the Ag(111) plasmon peak. This feature originates from interband transitions between states located on the hydrogen atoms and states on the Ag surface atoms.

DOI: [10.1103/PhysRevB.84.235430](https://doi.org/10.1103/PhysRevB.84.235430)

PACS number(s): 73.20.-r, 71.45.Gm, 71.15.-m

I. INTRODUCTION

A large part of the research in the emerging field of plasmonics focuses on designing the plasmonic properties of metallic structures through geometrical modifications on a subwavelength scale.¹ For example, the localized surface-plasmon resonances (LSPR) of noble-metal nanoparticles can be tuned by varying the size and shape of the particles.² The sensitivity of LSPR frequency to the surrounding dielectric environment forms the basis for molecular sensing.³⁻⁵ Despite the widespread use of this technique, the relation between the adsorbate-metal interaction and the plasmonic properties of the interface is not well understood. Recently, important advances in this direction were provided by electron-energy-loss measurements on well-characterized noble-metal surfaces. These measurements revealed a significant change in surface-plasmon energy and dispersion upon adsorption of thiol-bonded molecules, which was rationalized using qualitative arguments.⁶

Time-dependent density functional theory (TDDFT) has been successfully applied to describe plasmons in a wide range of materials, including simple metals and their surfaces,⁷ graphene-based materials,^{8,9} bulk transition metals,¹⁰ and even superconductors.¹¹ However, its application to noble-metal surfaces has remained a challenge. For the case of silver, which is one of the most commonly used materials for plasmonic applications, first-principles investigations have been performed for the bulk phase,¹² small,¹³ and medium¹⁴ silver clusters as well as atomic chains.¹⁵ However, *ab initio* calculations of plasmon excitations at Ag surfaces have so far not been reported. One of the known problems is the incorrect description of the Ag 3*d* bands by the local density approximation (LDA), which leads to an artificially large screening of the plasmons. The many-body GW method generally provides a good description of the *d* bands in noble metals such as Ag¹² and Cu.¹⁶ However, due to the computational cost, plasmon studies based on GW band structures have so far only been performed for the bulk phase of these metals.

In this work we take the first step toward a microscopic description of adsorbate-induced effects on metal surface plasmons by applying first-principles electronic structure theory to investigate how the plasmons of the Ag(111) surface are

modified by the adsorption of atomic hydrogen. The problem of the incorrect description of the Ag 3*d* bands with the LDA and similar (semi)local functionals is overcome by using the orbital-dependent GLLBSC (Gritsenko, Leeuwen, Lenthe, and Baerends potential¹⁷ with the modifications from Kuisma *et al.*¹⁸) functional. This functional lowers energy of the Ag 3*d* band by around 1 eV, leading to surface-plasmon energies for the Ag(111) surface in very good agreement with experiments. Furthermore, we find that, in the presence of hydrogen, the silver surface plasmon is redshifted by 0.1–0.2 eV and, in addition, a new peak arises at 0.6 eV below the surface-plasmon resonance. This new peak is shown to arise from interband transitions from the H atoms to the surface Ag atoms.

II. METHOD

All calculations have been performed by the grid-based projector augmented wave method (GPAW) code.^{19,20} The Ag(111) surface was modeled with 10 atomic layers (20.5 Å thick) and a 1 × 1 unit cell. A supercell containing 30-Å vacuum and a uniform grid spacing of 0.18 Å is used. The structure relaxation was carried out using LDA and 8 × 8 Monkhorst-Pack *k*-point sampling. The Kohn-Sham wave functions and band energies were calculated for the relaxed surface using both the LDA and the GLLBSC functional. The latter has recently been shown to produce band gaps for a range of different semiconductors, in very good agreement with experiments and more sophisticated theoretical approaches, while the computational cost is comparable to that of LDA.^{17,18}

The plasmon energies are obtained as peaks in the loss function, which is directly comparable to the electron-energy-loss spectroscopy (EELS). The former is defined as the imaginary part of the inverse dielectric function,

$$\text{Im}\epsilon^{-1}(\mathbf{q}, \omega) = V_c(\mathbf{q})\text{Im}\chi_{00}(\mathbf{q}, \omega), \quad (1)$$

where \mathbf{q} is a wave vector in the Brillouin zone (BZ) and $V_c(\mathbf{q}) = 4\pi/|\mathbf{q}|^2$ is the Coulomb interaction. $\chi_{GG'}(\mathbf{q}, \omega)$ is the wave vector and frequency-dependent density response function, which is calculated within the adiabatic local density approximation (ALDA) and using wave functions and single-particle energies from an LDA or GLLBSC calculation, respectively.

Since we consider a finite slab in a supercell geometry, \mathbf{q} is restricted to the two-dimensional (2D) surface BZ; i.e., its normal component is set to zero. In general, the loss function calculated in this way from Eq. (1) will show a peak both at the surface and bulk plasmon energies. An illustration of this can be seen in Fig. 2 of Ref. 22 for the case of a Mg slab. Details on the implementation of the response function in GPAW can be found in Ref. 22.

The density response function was calculated using the ALDA for exchange and correlation. To construct the density response function, a dense sampling of the surface Brillouin zone on a 100×100 Monkhorst-Pack k -point grid was used, and empty bands up to 30 eV above the Fermi level were included. A finite broadening parameter of 0.05 eV was introduced. Local field effects were included in the direction perpendicular to the surface with an energy cutoff of 500 eV. The thickness of the slab and vacuum, the grid spacing, the number of bands, and the effect of local fields were separately tested to ensure convergence of the plasmon energies to within 0.03 eV.

III. RESULTS

In Fig. 1 we show the band structure of the Ag(111) surface calculated with the LDA (grey) and the GLLBSC (black) functional. For the Ag(111) surface we find that GLLBSC shifts the top of the Ag d band down by around 1 eV compared to LDA, in good agreement with photoemission measurements on Ag films.²¹ The bottom of the d band is downshifted by 0.5 eV, leading to an effective narrowing of the d band of around 0.5 eV compared to LDA. The correction to the sp bands is found to be minimal. Similar GW corrections to the LDA band structure have been reported for bulk Ag¹² and Cu.¹⁶

Figure 2(a) shows the loss function of a clean Ag(111) surface calculated with LDA along the Γ - M direction of the surface Brillouin zone. The wave vectors increase from top to bottom in steps of $\Delta q = 0.025 \text{ \AA}^{-1}$. The peak at 2.9 eV corresponds to the surface-plasmon resonance. Due to the screening by the $3d$ electrons, this value is considerably redshifted relative to the homogeneous electron gas prediction of 6.4 eV.²³ However, due to the high position of the $3d$ band in LDA (see Fig. 1) the screening is overestimated, and the plasmon energy obtained is too low compared to the

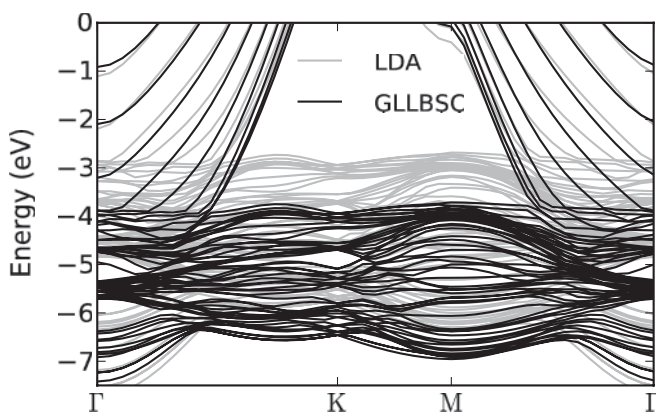


FIG. 1. The band structure of the Ag(111) surface calculated with LDA (grey) and GLLBSC (black). The Fermi energy is set to zero.

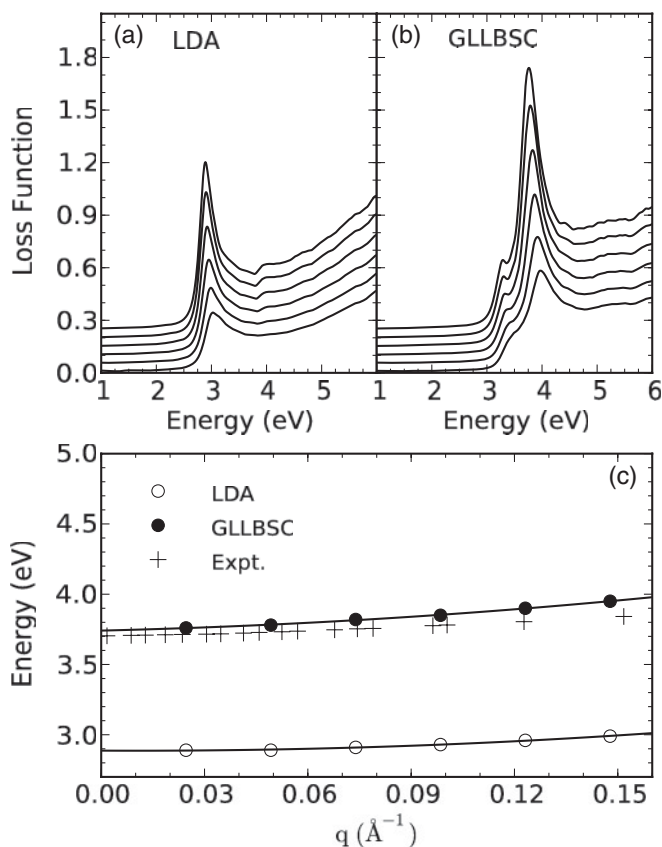


FIG. 2. Electron-energy-loss functions for the Ag(111) surface calculated with (a) LDA and (b) GLLBSC, respectively. (c) The corresponding surface-plasmon dispersions, shown together with experimental values extracted from Ref. 24. Lines in (c) are added to guide the eye.

experimental value of 3.71 eV.²⁴ Similar failures have been reported for other bulk noble metals such as gold and copper.²⁵

Figure 2(b) shows the loss functions obtained from the wave functions and energies of a GLLBSC calculation. The better description of the Ag $3d$ states significantly improves the surface-plasmon energy. In Fig. 2(c) we compare the calculated q -dependent plasmon energies with experimental values reported by Moresco *et al.*²⁴ The GLLBSC values are in remarkably good agreement with the experiments with deviations less than 0.15 eV in the considered wave-vector range. While the GLLBSC improves the plasmon energies, the width of the resonance remains too large. In fact, the experimental EELS shows a very intense peak with a width around 0.1 eV, while both GLLBSC and LDA yield a less intense peak with a width of 0.5 eV. Since we perform calculations for a ten-layer Ag slab, one might expect to see also the bulk plasmon in the EELS spectrum. However, for silver the deviation between the surface and bulk plasmon energies is only 0.1 eV. Since this energy difference is smaller than the width of the plasmon peak, we do not resolve two peaks. On the other hand, our calculations for the Mg(0001) surface show that, while the surface plasmon is converged for 10 layers, the bulk plasmon peak only emerges for slabs thicker than 16 layers.²²

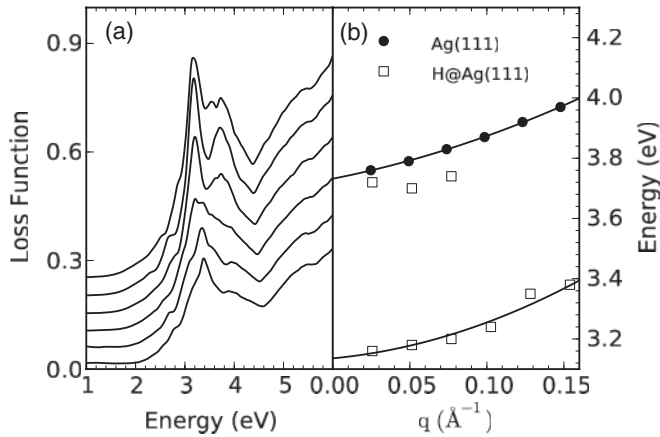


FIG. 3. (a) Energy-loss functions for the Ag(111) surface covered by a monolayer of hydrogen. (b) The corresponding dispersion relations (open squares) compared with that of the clean surface (solid circles). Lines in (b) are added to guide the eye.

We next consider the effect of a simple adsorbate on the surface plasmons. Figure 3(a) shows the loss function of a ten-layer slab of Ag(111) covered by a monolayer of H atoms on both sides of the slab. The q vector increases in steps of $\Delta q = 0.025 \text{ \AA}^{-1}$ from top to bottom. In contrast to the single sharp surface-plasmon resonance found for the clean surface in Fig. 2(b), two peaks with considerably lowered strengths are visible in the energy range 2–5 eV. As q increases, both peaks disperse toward higher energies but show distinct damping behavior. The strength of the high-energy peak decays much faster than that of the lower-energy peak. The energies of both peaks are plotted in Fig. 3(b) as a function of q . The high-energy branch is quite close to that of the clean surface (black dots), indicating that this feature is due to a modified version of the original Ag(111) surface plasmon. Interestingly, the adsorption of hydrogen changes the dispersion of this plasmon in the low- q regime from positive to negative. The same behavior (change from positive to negative dispersion) was observed experimentally for the surface plasmon of Au(111) upon adsorption of thiolate-bonded molecules.⁶ Since a negative dispersion is characteristic of free-electron metals, this change can be explained by a reduced effect of screening by the Ag $4d$ electrons at the surface when the H atoms are adsorbed, i.e., the H atoms make the surface more free-electron-like.²³ The low-energy peak in the loss spectrum of H/Ag(111) is around 0.6 eV lower than the surface plasmon of the clean Ag(111) surface. This suggests that the origin of this feature is qualitatively different from the original surface plasmon of Ag(111).

In general, the effect of adsorbates on the surface collective excitations may be divided into a “static” contribution arising from hybridization and charge transfer at the interface and a “dynamic” contribution arising from the screening response of the electron system. The latter effect is, e.g., responsible for the damping of plasmons in adsorbed graphene²⁶ and the narrowing of the energy gap of molecules weakly physisorbed on a surface.²⁷ To distinguish the two effects, the loss function was calculated with the hydrogen layer gradually moving away from the Ag surface. When the hydrogen atoms are more

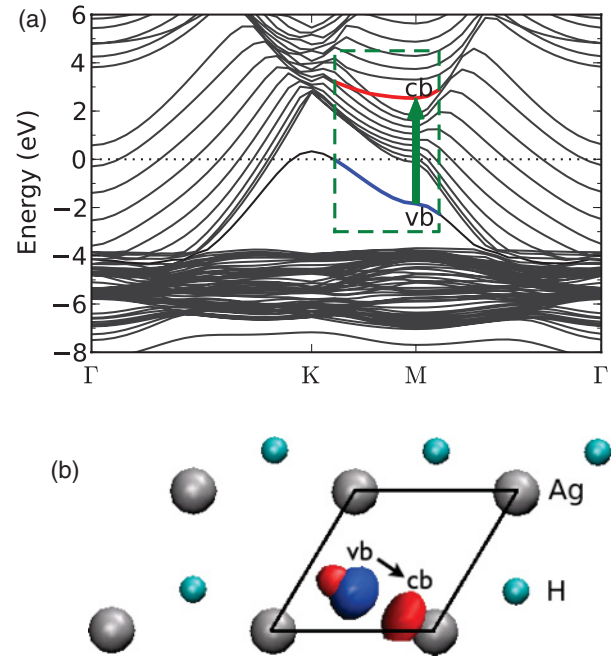


FIG. 4. (Color online) (a) Band structure of the Ag(111) surface with a monolayer of hydrogen. The low-energy peaks in Fig. 3(a) are dominated by transitions between the vb (blue) and cb (red) bands. The dotted line at zero indicates the Fermi level. (b) The wave function of the occupied vb (blue) and unoccupied cb (red) band that is responsible for the above interband transitions. The black lines indicate the unit cell.

than 2 \AA away from the surface, hybridization and charge-transfer effects are negligible. At this distance the low-energy peak completely disappears from the loss spectrum, and the higher-energy peak becomes identical to the surface-plasmon resonance of a clean Ag surface. This shows that the high-energy peak is indeed a modified surface plasmon of the Ag surface, while the low-energy peak originates from a change of the electronic band structure and wave functions at the interface, i.e., a static effect.

To further analyze the origin of the low-energy peak, we note that the loss function (in the low- q limit) can be written as $\epsilon_2(\omega)/[\epsilon_1(\omega)^2 + \epsilon_2(\omega)^2]$, where ϵ_1 and ϵ_2 are the real and imaginary parts of the macroscopic dielectric function, respectively. Because local field effects are in fact negligible for small q , ϵ_2 is simply a joint density of states of vertical single-particle transitions weighted by dipole matrix elements, i.e., it has peaks at $|\epsilon_{m\mathbf{k}+\mathbf{q}} - \epsilon_{n\mathbf{k}}|$ with magnitude $|\langle \psi_{n\mathbf{k}} | e^{-i\mathbf{q}\cdot\mathbf{r}} | \psi_{m\mathbf{k}+\mathbf{q}} \rangle|^2$, where $\epsilon_{n\mathbf{k}}$ and $\psi_{n\mathbf{k}}$ are the Kohn-Sham eigenenergy and wave function at band n with wave vector \mathbf{k} . We find that $\epsilon_2(\omega)$ (not shown) has a peak at the same energy as the low-energy peak in the loss spectrum. This shows that the low-energy peak is not due to a plasmon in the usual sense [characterized by $\epsilon(\omega) = 0$] but is rather due to a high density of uncorrelated single-particle transitions. In Fig. 4(a) we show the interband transitions that give rise to the peak. Note that the usual condition of a surface plasmon $\epsilon(\omega) + 1 = 0$ is (approximately) valid when ϵ is the bulk permittivity. In our case ϵ is the dielectric function of the interface, and thus $\epsilon(\omega) = 0$ is the correct condition.

The transitions giving rise to the low-energy peak in the loss spectrum occur between the bands marked by the vb (blue) and cb (red) curves in Fig. 4(a). These two bands are absent in the band structure of the clean surface but emerge from the adsorption of the hydrogen monolayer. Figure 4(b) shows the shape of the wave functions corresponding to the states marked by the arrow in Fig. 4(a). The occupied band [indicated with vb in Fig. 4(a) and 4(b)] has an *s*-orbital shape and is located on the hydrogen atom (small cyan spheres). The unoccupied band [indicated with cb] has *p*-orbital character and is mainly located on the surface Ag atom (large grey spheres). We thus conclude that the low-energy peak in the loss spectrum of Fig. 3 originates from the interband transitions from the H atoms to the surface Ag atoms. These interband transitions also act as a decay channel for the modified surface plasmon (the high-energy peak), explaining the stronger damping of the latter as compared to the clean surface plasmon.

IV. CONCLUSIONS

In conclusion, we have calculated the electron-energy-loss spectrum of a Ag(111) surface with and without a hydrogen

monolayer using TDDFT linear-response theory. An accurate description of the Ag *3d* bands was found to be crucial for quantitative agreement with experiments for the surface plasmons of clean surface. Upon adsorption of hydrogen a new low-energy peak emerges in the EELS spectrum. The new feature was attributed to interband transitions from a band located mainly on the H atoms to a band located on the surface Ag atoms. These results show that the surface plasmons of noble-metal surfaces can be significantly modified by adsorbate molecules.

ACKNOWLEDGMENTS

The Center for Atomic-scale Materials Design is sponsored by the Lundbeck Foundation. The Catalysis for Sustainable Energy initiative is funded by the Danish Ministry of Science, Technology and Innovation. The computational studies were supported as part of the Center on Nanostructuring for Efficient Energy Conversion, an Energy Frontier Research Center funded by the US Department of Energy, Office of Science, Office of Basic Energy Sciences under Award No. DE-SC0001060.

*thygesen@fysik.dtu.dk

¹S. A. Maier, *Plasmonics: Fundamentals and Applications* (Springer, New York, 2007).

²K. L. Kelly, E. Coronado, L. L. Zhao, and G. C. Schatz, *J. Phys. Chem. B* **107**, 668 (2003).

³S. M. Morton, D. W. Silverstein, and L. Jensen, *Chem. Rev.* **111**, 3962 (2011).

⁴E. M. Larsson, C. Langhammer, I. Zori, and B. Kasemo, *Science* **326**, 1091 (2009).

⁵K. A. Willets and R. P. Van Duyne, *Annu. Rev. Phys. Chem.* **58**, 267 (2007).

⁶S. J. Park and R. E. Palmer, *Phys. Rev. Lett.* **102**, 216805 (2009).

⁷J. M. Pitarke, V. M. Silkin, E. V. Chulkov, and P. M. Echenique, *Rep. Prog. Phys.* **70**, 1 (2007).

⁸A. G. Marinopoulos, L. Reining, V. Olevano, and A. Rubio, *Phys. Rev. Lett.* **89**, 076402 (2002).

⁹R. Hambach, C. Giorgetti, F. Sottile, L. Reining, N. Hiraoka, Y. Q. Cai, A. G. Marinopoulos, and F. Bechstedt, *Phys. Rev. Lett.* **101**, 266406 (2008).

¹⁰I. G. Gurtubay, J. M. Pitarke, W. Ku, A. G. Eguiluz, B. C. Larson, J. Tischler, P. Zschack, and K. D. Finkelstein, *Phys. Rev. B* **72**, 125117 (2005).

¹¹W. Ku, W. E. Pickett, R. T. Scalettar, and A. G. Eguiluz, *Phys. Rev. Lett.* **88**, 057001 (2002).

¹²A. Marini, R. Del Sole, and G. Onida, *Phys. Rev. B* **66**, 115101 (2002).

¹³J. C. Idrobo, S. Ögüt, and J. Jellinek, *Phys. Rev. B* **72**, 085445 (2005).

¹⁴C. M. Aikens, S. Li, and G. C. Schatz, *J. Phys. Chem. C* **112**, 11272 (2008).

¹⁵J. Yan and S. Gao, *Phys. Rev. B* **78**, 235413 (2008).

¹⁶A. Marini, G. Onida, and R. Del Sole, *Phys. Rev. Lett.* **88**, 016403 (2001).

¹⁷O. Gritsenko, R. van Leeuwen, E. van Lenthe, and E. J. Baerends, *Phys. Rev. A* **51**, 1944 (1995).

¹⁸M. Kuisma, J. Ojanen, J. Enkovaara, and T. T. Rantala, *Phys. Rev. B* **82**, 115106 (2010).

¹⁹J. J. Mortensen, L. B. Hansen, and K. W. Jacobsen, *Phys. Rev. B* **71**, 035109 (2005).

²⁰J. Enkovaara *et al.*, *J. Phys. Condens. Matter* **22**, 253202 (2010).

²¹N. J. Speer *et al.*, *Europhys. Lett.* **88**, 67004 (2009).

²²J. Yan, J. J. Mortensen, K. W. Jacobsen, and K. S. Thygesen, *Phys. Rev. B* **83**, 245122 (2011).

²³A. Liebsch, *Phys. Rev. Lett.* **71**, 145 (1993).

²⁴F. Moresco, M. Rocca, V. Zielasek, T. Hildebrandt, and M. Henzler, *Surf. Sci.* **388**, 24 (1997).

²⁵V. P. Zhukov, F. Aryasetiawan, E. V. Chulkov, I. G. de Gurtubay, and P. M. Echenique, *Phys. Rev. B* **64**, 195122 (2001).

²⁶J. Yan, K. S. Thygesen, and K. W. Jacobsen, *Phys. Rev. Lett.* **106**, 146803 (2011).

²⁷K. S. Thygesen and A. Rubio, *Phys. Rev. Lett.* **102**, 046802 (2009).